

# Compounds of Group 14 Elements with an Element–Element (E = Si, Ge, Sn) Bond: Effect of the Nature of the Element Atom

Kirill V. Zaitsev,<sup>\*,†</sup> Elmira Kh. Lermontova,<sup>‡</sup> Andrei V. Churakov,<sup>‡</sup> Viktor A. Tafeenko,<sup>†</sup> Boris N. Tarasevich,<sup>†</sup> Oleg Kh. Poleshchuk,<sup>§,||</sup> Anastasia V. Kharcheva,<sup>†</sup> Tatiana V. Magdesieva,<sup>†</sup> Oleg M. Nikitin,<sup>†,⊥</sup> Galina S. Zaitseva,<sup>†</sup> and Sergey S. Karlov<sup>†</sup>

<sup>†</sup>Department of Chemistry, Moscow State University, Leninskiye Gory, 1, Moscow 119991, Russia

<sup>‡</sup>N. S. Kurnakov General and Inorganic Chemistry Institute, Russian Academy of Science, Leninskii Pr., 31, Moscow 119991, Russia

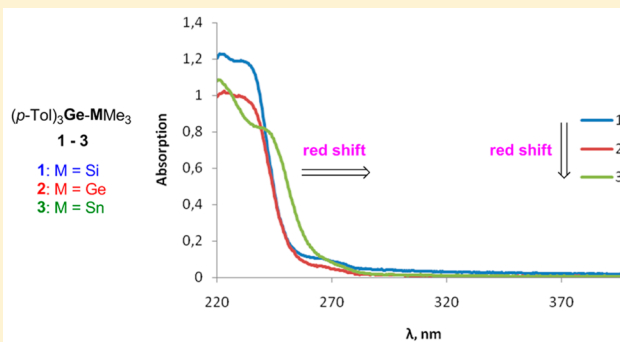
<sup>§</sup>National Research Tomsk Polytechnic University, Lenin Av., 30, Tomsk 634050, Russia

<sup>||</sup>Tomsk State Pedagogical University, Kievskaya Str., 60, Tomsk 634061, Russia

<sup>⊥</sup>A. N. Nesmeyanov Institute of Organoelement Compounds, Russian Academy of Science, Vavilova Str. 28, Moscow 119991, Russia

## Supporting Information

**ABSTRACT:** Two series of germanium compounds, (*p*-Tol)<sub>3</sub>Ge-MMe<sub>3</sub> (M = Si (1), Ge (2), Sn (3)) and (Me<sub>3</sub>Si)<sub>3</sub>Ge-MPh<sub>3</sub> (M = Ge (4), Sn (5)), were prepared using lithium or potassium intermediates. The changing of the reaction conditions results in trigermane Ph<sub>3</sub>Ge-Ge(SiMe<sub>3</sub>)<sub>2</sub>-GePh<sub>3</sub> (6). The molecular structures of 1, 2, and 6 were investigated by X-ray analysis. By UV/visible spectroscopy it is established that introduction of a tin atom results in a significant bathochromic absorption shift. Furthermore, according to cyclic voltammetry, oxidation potentials decrease in the order 1 > 2 > 3. The electronic structures of 1–4 and related (Me<sub>3</sub>Si)<sub>3</sub>Ge-SiPh<sub>3</sub> were investigated by DFT calculations. Fluorescence properties of 1–3 were studied in the solid state and in solution; for compound 3 phosphorescence (lifetime is 4.58 ms) is observed in the solid state.



## INTRODUCTION

Oligosilanes, oligogermanes, and oligostannanes are the heavy analogues of the hydrocarbons. A distinctive feature of these compounds is the effective overlap of hybridized atomic orbitals of the neighbor elements that leads to the sharing of the electron density along the entire chain of bonded Si, Ge, or Sn atoms ( $\sigma$ -delocalization). This in turn results in the appearance of the properties typical for unsaturated hydrocarbons (intense absorption in the UV region, thermochromism, nonlinear optical properties, luminescence, conductivity, etc.).<sup>1</sup>

In this regard, well-defined oligogermanes in the nanometer scale could be potentially useful molecular models to understand the photophysical properties of germanium nanostructures.

Optical, electronic, and electrochemical properties of the oligomeric compounds of a given type depend on the number of E (E = Si, Ge, or Sn) atoms in the chain, on the nature of the substituents (electron-donating and/or electron-withdrawing), and on the structure of the molecule.<sup>2</sup>

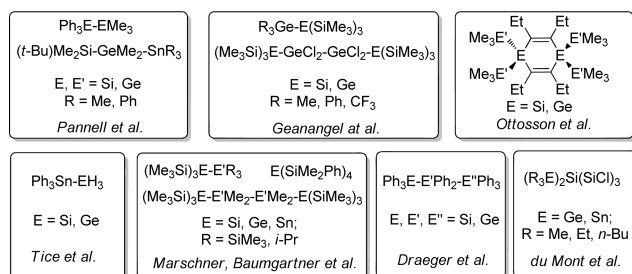
At the same time, the obvious difficulties in oligogermane synthesis (low yields, the mixtures of byproducts, low selectivity) as well as the high cost of the starting compounds are observed. From this point of view it is particularly interesting to investigate (by UV/visible spectroscopy, electro-

chemical methods, emission spectroscopy) the change of  $\sigma$ -conjugation in oligogermanes by replacing germanium atoms with silicon or tin. Investigation of the UV absorption of such compounds is an important procedure for describing the properties of the studied derivatives.

It should be noted that there are only a limited number of publications in which the structure and properties (including UV/visible absorbance) of the catenated compounds of group 14 elements containing different atoms (Si, Ge, Sn) have been investigated (Chart 1; see references below).<sup>3</sup>

In this work in order to investigate the effect of Si, Ge, and Sn atoms in germanium compounds, we carried out the synthesis of a series of germanium-containing compounds, (*p*-Tol)<sub>3</sub>Ge-MMe<sub>3</sub> (1–3; M = Si, Ge, Sn) and (Me<sub>3</sub>Si)<sub>3</sub>Ge-MPh<sub>3</sub> (4, 5; M = Ge, Sn). Also on changing the synthesis conditions, compound 6, (Me<sub>3</sub>Si)<sub>2</sub>Ge(GePh<sub>3</sub>)<sub>2</sub>, was obtained. The structures of all compounds were investigated in solution by multinuclear NMR spectroscopy and in the case of 1, 2, and 6 in the solid state by X-ray analysis. Compounds 1–3 were investigated by electrochemical methods and fluorescence emission spectroscopy. It was established that introduction of

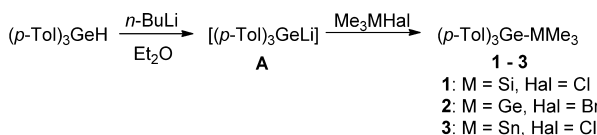
Received: December 17, 2014

**Chart 1. Structures of Catenated Germanium Compounds Containing Silyl or Stannyl Groups**

Sn groups in germanium compounds results in a significant bathochromic shift in the UV absorption, and the oxidation potentials decrease in the order Si > Ge > Sn derivatives. The fluorescence spectra depend on state of the substance studied (powder or solution), and in the case of a Sn-containing germane a red-shifted band is also observed.

## RESULTS AND DISCUSSION

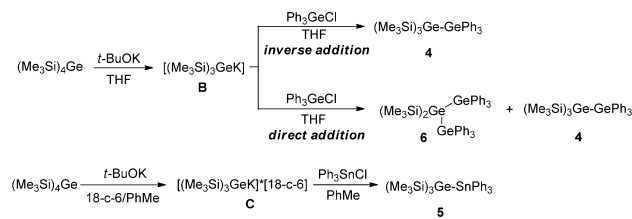
**Synthesis.** In this work the target compounds were obtained via the reaction of *in situ* generated alkali metal derivatives of Ge compounds with corresponding halogenides. Compounds 1–3, containing a *p*-tolyl group, were obtained using triarylgermyllithium derivative **A** and alkyl derivatives of Si, Ge, and Sn (Scheme 1).

**Scheme 1. Synthesis of Compounds 1–3**

According to NMR spectroscopy data, compounds 1–3 have very similar spectra. In the <sup>1</sup>H NMR spectra (CDCl<sub>3</sub>, RT) there are two doublets for the AB system of aromatic protons for *p*-MeC<sub>6</sub>H<sub>4</sub> (7.21, 7.14, 7.17 and 7.39, 7.30, 7.33 ppm, respectively, <sup>3</sup>J<sub>H-H</sub> = 7.8 Hz) and singlets of methyl groups for *p*-MeC<sub>6</sub>H<sub>4</sub> (2.41, 2.34, 2.37 ppm, respectively) and for MMe<sub>3</sub> groups (0.38, 0.39, 0.30 ppm, respectively). At the same time, the more significant differences are observed in the <sup>13</sup>C NMR spectra (CDCl<sub>3</sub>, RT). Thus, the signals for the MMe<sub>3</sub> group (−0.33, −0.86, −9.76 ppm, respectively) are significantly shifted to the high field in the range of the Si, Ge, and Sn derivatives. This fact may be explained by the decreasing of ionization energies in the element range.

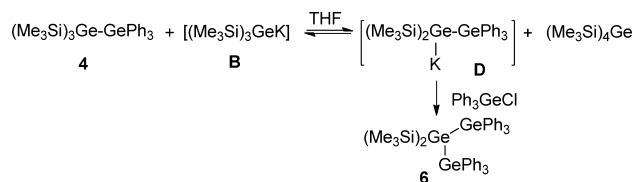
Substances 4–6 were obtained using the reaction of potassium compounds **B** and **C** with triaryl derivatives of Ge and Sn (Scheme 2). It should be noted that this is the first time for the application of intermediates **B** and **C** in reactions with aryl derivatives of group 14 elements.

It was established that in this interaction the different products have been formed depending on the order of addition of reactants. Thus, inverse addition (addition of **B** to the diluted solution of Ph<sub>3</sub>GeCl in THF) results in digermene **4** in good yield. On the contrary, direct addition (addition of a diluted solution of Ph<sub>3</sub>GeCl in THF to **B**) gives a mixture of trigermene **6** (main product) and **4**, which may be separated by column chromatography. It should be noted that compound **6**

**Scheme 2. Synthesis of Compounds 1–3**

is the first example of a linear trigermene containing two silyl groups.

Obviously, compound **6** was formed from **4** with a local excess of **B** in a slow reaction (Scheme 3). The presence of byproduct (Me<sub>3</sub>Si)<sub>4</sub>Ge may be detected by NMR spectroscopy of the crude reaction mixture.

**Scheme 3. Possible Mechanism for the Synthesis of Compound 6**

It is evident that the synthesis of compound **6** may pass from **4** through formation of the intermediate **D**.

The successful synthesis of compound **5** without scrambling of groups along the element chain may be explained by introducing voluminous Me<sub>3</sub>Si groups. Such stabilization in the case of related Ge<sup>4</sup> or Sn<sup>3e,g</sup> compounds was observed earlier.

The data of the NMR spectra for (Me<sub>3</sub>Si)<sub>3</sub>Ge-SiPh<sub>3</sub>,<sup>3b</sup> **4**, and **5** are very similar, too. At the same time the signals in the <sup>29</sup>Si NMR spectra (−4.9, −4.35, −2.68 ppm, respectively) are somewhat shifted to low field in the range of the Si, Ge, and Sn compounds. This fact may be explained by the presence of phenyl groups conjugated with M; a similar shift was observed earlier for related compounds under introduction of electron-withdrawing groups.<sup>3d,5</sup> Anyway the fact observed indicates the participation (although weak) of trimethylsilyl groups in conjugation along the group 14 elements.<sup>3j</sup>

**X-ray Crystallographic Study.** In this work the molecular structures of three compounds were investigated by single-crystal X-ray analysis (Figures 1–3; Table S1, Supporting Information).

It should be noted that to date only three compounds containing an Ar<sub>3</sub>Ge-SiAlk<sub>3</sub> fragment have been studied by XRD (Chart 2).<sup>6,7</sup>

In general the structural parameters of **1** are very close to those of Ph<sub>3</sub>Ge-SiMe<sub>3</sub>,<sup>6</sup> and so the structural parameters in compounds of such type slightly depend on the changing aromatic substituents at the Ge atom. At the same time **1** crystallizes in the monoclinic P2<sub>1</sub>/c space group, unlike Ph<sub>3</sub>Ge-SiMe<sub>3</sub>, which crystallizes in the trigonal P<sup>3</sup> space group.

In structure **1** silicon and germanium atoms adopt a distorted tetrahedral environment. The substituents are in the skewed (*gauche*) conformation (torsion angle C–Ge–Si–C 75.50(12)°).

To date there are only seven structures of digermenes of the type Ar<sub>3</sub>Ge-GeAlk<sub>3</sub> that have been studied by X-ray analysis (Chart 3).<sup>8</sup>

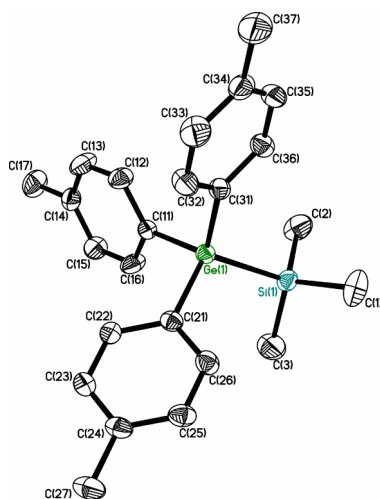


**Figure 1.** Molecular structure of **1**. Displacement ellipsoids are shown at the 50% probability level. Hydrogen atoms are omitted for clarity. Selected bond lengths (Å) and bond angles (deg): Ge(1)–Si(1) 2.3892(5), Ge(1)–C<sub>av</sub> 1.9559(7), Si(1)–C<sub>av</sub> 1.867(2); C–Ge(1)–C<sub>av</sub> 107.41(7), C–Ge(1)–Si(1)<sub>av</sub> 111.41(5), C–Si(1)–C<sub>av</sub> 109.03(12), C–Si(1)–Ge(1) 109.91(7).

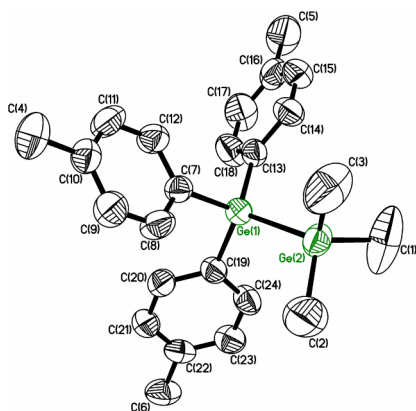


**Figure 2.** Molecular structure of **2**. Displacement ellipsoids are shown at the 40% probability level. Hydrogen atoms are omitted for clarity. Selected bond lengths (Å) and bond angles (deg): Ge(1)–Ge(2) 2.4292(7), Ge(1)–C<sub>av</sub> 1.948(4), Ge(2)–C<sub>av</sub> 1.936(7); C–Ge(1)–C<sub>av</sub> 107.97(17), C–Ge(1)–Ge(2)<sub>av</sub> 110.90(12), C–Ge(2)–C<sub>av</sub> 107.2(4), C–Ge(2)–Ge(1)<sub>av</sub> 115.6(2).

In (*p*-Tol)<sub>3</sub>Ge–GeMe<sub>3</sub> (**2**) both Ge atoms have a distorted tetrahedral environment, and the geometry at the aryl-substituted Ge atom is more distorted. Furthermore, the Ge–C bond lengths with *p*-Tol are somewhat elongated in comparison with aliphatic (Me) groups. From comparison of the structural parameters for **2** and structures presented in Chart 1, it is evident that the steric volume of the alkyl substituents has a major effect on Ge–Ge bond length. The Ge–Ge bond length in **2** is increased in comparison with the previously described aryl-substituted compounds (compare 2.4292(7) Å in **2** vs 2.408(1) Å<sup>9</sup> in (*p*-Tol)<sub>3</sub>Ge–GePh<sub>3</sub>, and vs 2.419(1) Å<sup>10</sup> in (*p*-Tol)<sub>3</sub>Ge–Ge(*p*-Tol)<sub>3</sub>), indicating an influence of electronic factors on the digermene structure. Apparently, the aromatic substituents at Ge support the conjugation between germanium atoms (see Theoretical Calculations below). The substituents in the Ge–Ge fragment are in the *gauche*-conformation (torsion angle C–Ge–Ge–C<sub>av</sub>

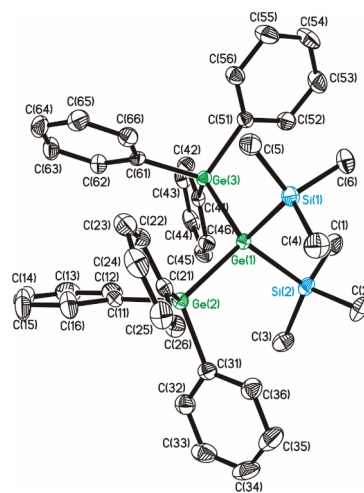


**Figure 3.** Molecular structure of **6**. Displacement ellipsoids are shown at the 50% probability level. Hydrogen atoms are omitted for clarity. Selected bond lengths (Å) and bond angles (deg): Ge(1)–Si(1) 2.4037(6), Ge(1)–Si(2) 2.4184(6), Ge(1)–Ge(2) 2.4494(3), Ge(1)–Ge(3) 2.4526(3), Ge(2)–C<sub>av</sub> 1.958(2), Ge(3)–C<sub>av</sub> 1.962(2), Si(1)–C<sub>av</sub> 1.871(2), Si(2)–C<sub>av</sub> 1.870(2); Si(1)–Ge(1)–Si(2) 104.78(2), Si(1)–Ge(1)–Ge(2) 109.456(17), Si(2)–Ge(1)–Ge(2) 110.610(17), Si(1)–Ge(1)–Ge(3) 107.039(17), Si(2)–Ge(1)–Ge(3) 112.654(16), Ge(2)–Ge(1)–Ge(3) 111.949(10), C–Ge(2)–C<sub>av</sub> 106.97(9), C–Ge(2)–Ge(1)<sub>av</sub> 111.89(6), C–Ge(3)–C<sub>av</sub> 106.56(8), C–Ge(3)–Ge(1)<sub>av</sub> 112.21(6).

## Chart 2. Structures of Germanium Compounds of the Type Ar<sub>3</sub>Ge–SiAlk<sub>3</sub> Investigated by X-ray Analysis

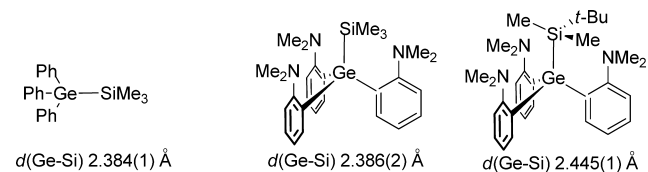
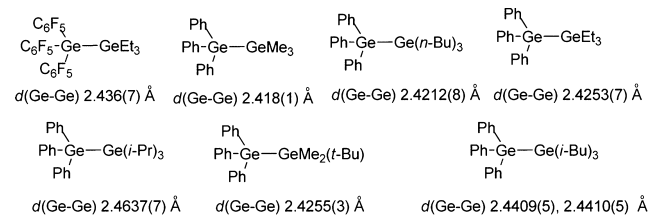


## Chart 3. Structures of Germanium Compounds of the Type Ar<sub>3</sub>Ge–GeAlk<sub>3</sub> Investigated by X-ray Analysis

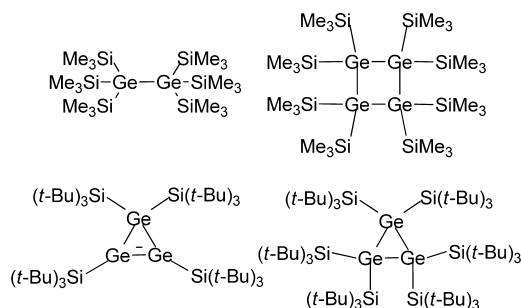


79.46(4)°). It should be noted that compounds **1** and **2** are isostructural.

In comparing the structural data of **1** and **2**, it is evident that a change in the nature of the element in the chain (GeMe<sub>3</sub> vs SiMe<sub>3</sub>) has an insignificant effect on the structural parameters of the Ge(*p*-Tol)<sub>3</sub> fragment and the molecule as a whole.

It should be noted that compound **6** represents the first example of a linear germane containing two silyl substituents at one Ge atom investigated by X-ray analysis. Nowadays there are only cyclic structures of this type (Chart 4).<sup>3k,11</sup>

The geometry of all Ge atoms in **6** may be described as distorted tetrahedral. The main feature of **6** is the increased value of the Ge–Ge–Ge angle in relation to the Si–Ge–Si angle (104.78(2)° vs 111.949(10)°), which is typical for

**Chart 4. Structures of Oligogermanes Containing Silyl Substituents Investigated by X-ray Analysis**

nontransition elements (Bent's rule).<sup>17</sup> At the same time this structural feature indicates that the Si atoms in this molecule are only slightly included in the conjugation with the oligogermanium chain (see UV/Visible Spectroscopy below). The other structural parameters of **6** (for example, the Ge–C bond length) are close to related trigermanes (Table 1). It should be noted that nowadays there are only nine structures of linear trigermanes investigated by X-ray analysis.

**Table 1. Comparison of Structural Parameters of Trigermanes Investigated by X-ray Analysis**

compound	$d(\text{Ge}-\text{Ge}), \text{\AA}$	$d(\text{Ge}-\text{C})_{\text{av}}, \text{\AA}$	angle Ge–Ge–Ge, deg	ref
$\text{Ph}_3\text{Ge}-\text{GePh}_2-\text{GePh}_3$	2.438(2), 2.441(2)	1.96(1)	121.3(1)	12
$\text{Ph}_3\text{Ge}-\text{GeMe}_2-\text{GePh}_3$	2.429(1)	1.951(6)	120.3(1)	13
$\text{ClPh}_2\text{Ge}-\text{GePh}_2-\text{GePh}_2\text{Cl}$	2.413(2), 2.419(2), 2.423(2), 2.437(2)	1.950(2)	116.7(1), 110.4(1)	14
$(p\text{-Tol})_3\text{Ge}-\text{GePh}_2-\text{Ge}(p\text{-Tol})_3$	2.4318(5), 2.4338(4)	1.955(3)	114.80(2)	9
$(p\text{-Tol})_3\text{Ge}-\text{Ge}(p\text{-Tol})_2-\text{Ge}(p\text{-Tol})_3$	2.4359(5), 2.4450(4)	1.954(2)	117.54(1)	9
$\text{I}(t\text{-Bu})_2\text{Ge}-\text{Ge}(t\text{-Bu})_2-\text{Ge}(t\text{-Bu})_2\text{I}$	2.622(1), 2.660(1)	2.054(1)	115.4(1)	15
$\text{Br}(t\text{-Bu})_2\text{Ge}-\text{Ge}(t\text{-Bu})_2-\text{Ge}(t\text{-Bu})_2\text{Br}$	2.623(1), 2.595(1)	2.050(6)	113.5(1)	16
$\text{Me}(t\text{-Bu})_2\text{Ge}-\text{Ge}(t\text{-Bu})_2-\text{Ge}(t\text{-Bu})_2\text{Me}$	2.620(1)	2.027(7)	118.6(1)	16
$(p\text{-Tol})_3\text{Ge}-\text{Ge}(\text{C}_6\text{F}_5)_2-\text{Ge}(p\text{-Tol})_3$	2.459(5)	1.970(4)	124.10(3)	4
$(\text{Me}_3\text{Si})_3\text{Ge}-\text{GeMe}_2-\text{Ge}(\text{SiMe}_3)_3$	2.4616(8)	1.979(6)	125.00(4)	3b

According to this data, the presence of sterically large  $\text{Me}_3\text{Si}$  groups in **6** results in one of the smallest Ge–Ge–Ge angles ( $111.95^\circ$ ) and some elongation of the Ge–Ge bond (in comparison with  $[\text{Ph}_3\text{Ge}]_2\text{GeMe}_2$  and  $[\text{Ph}_3\text{Ge}]_2\text{GePh}_2$ ).

**UV/Visible Spectroscopy.** Oligomeric compounds of this type are characterized by an intense absorption band in the UV/visible spectrum ( $\epsilon$  exceeds  $10^4 \text{ cm}^{-1} \text{ M}^{-1}$ ) due to the allowed electronic transition. According to the analysis of the molecular orbitals, the highest occupied molecular orbital (HOMO) to a greater extent localized along the chain of atoms and may be regarded as a  $\sigma$ -bonding orbital formed by overlapping hybrid orbitals of each atom of silicon, germanium, or tin.<sup>18</sup> The lowest unoccupied molecular orbital (LUMO) in the absence of aromatic substituents also localized between the E atoms (E = Si, Ge, Sn) and may be regarded as a  $\sigma^*$ -

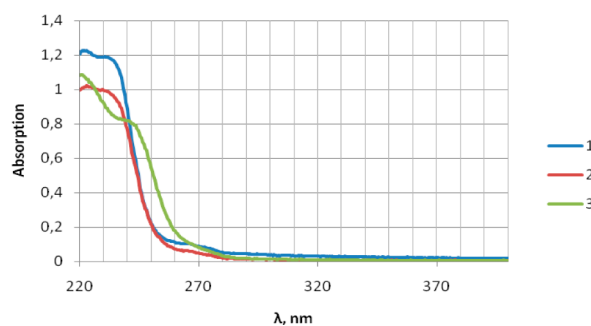
antibonding orbital. Thus, in the case of compounds with element–element bonds that contain only aliphatic substituents, the absorption band in the UV/visible spectrum corresponds to a  $\sigma \rightarrow \sigma^*$  transition.

In general, the energy gap is determined by many factors, including the nature of the substituent at Si, Ge, and Sn in the oligomeric chain, conformation of the molecule (*anti*-conformation leads to more effective  $\sigma$ -delocalization<sup>19</sup>), and the number of bonded element atoms in the chain. Now it is evident that increasing the amount of conjugated atoms causes a more significant bathochromic shift.

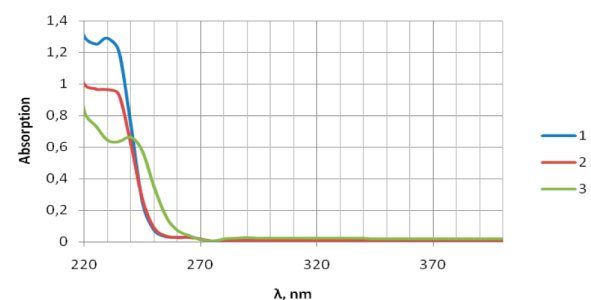
With the introduction of aromatic substituents with an intrinsic  $\pi$ -system, the LUMO moves to the carbon atoms of the phenyl rings, which actually becomes an antibonding  $\pi^*$ -orbital. The transition  $\sigma \rightarrow \pi^*$  is forbidden by orbital symmetry, but the band in the UV/visible absorption spectra does not disappear. Apparently, this suggests involvement of the HOMO–1 and/or LUMO+1 molecular orbitals; that is, in this case the  $\sigma \rightarrow \sigma^*$  transition also occurs. It should be noted that the additional bands (electron  $\pi \rightarrow \pi^*$  transitions) typical for aromatic substituents are weaker and overlap with more intense bands or appear as a shoulder to the corresponding peak.

The phenyl substituent is a good  $\sigma$ -donor and increases the electron density at the HOMO. Introduction of electron-withdrawing substituents results in LUMO destabilization.<sup>4</sup> This leads to a bathochromic shift of the absorption band.<sup>8e,20</sup>

The experimental UV spectral data for compounds **1–6** (Figures 4–7) and related known derivatives are collected in

**Figure 4.** UV spectra for **1–3** in  $\text{CH}_2\text{Cl}_2$ .

Tables 2, 3. The spectra were registered in  $\text{CH}_2\text{Cl}_2$  and *n*-hexane. It should be noted that the solvent affects the form of the absorption spectra to a small degree, but in *n*-hexane the absorption is more intense.

**Figure 5.** UV spectra for **1–3** in *n*-hexane.

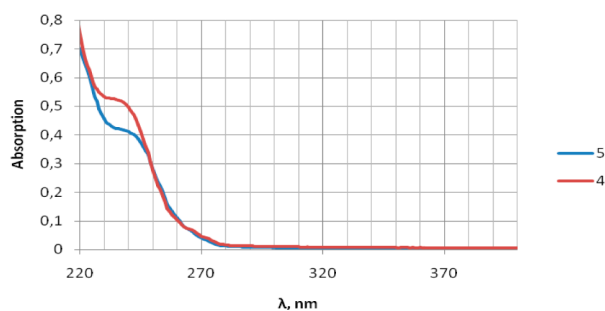


Figure 6. UV spectra for 4 and 5 in *n*-hexane.

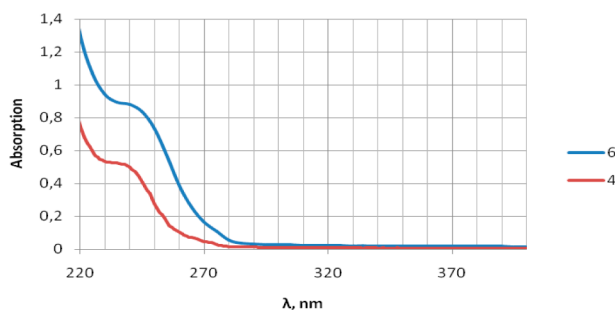


Figure 7. UV spectra for 4 and 6 in *n*-hexane.

Table 2. Data of the UV Spectroscopy for 1–6 (in *n*-Hexane) and Related Compounds

compound	$\lambda_{\text{max}}$ nm ( $\epsilon \times 10^{-4}$ , M <sup>-1</sup> cm <sup>-1</sup> )	ref
1 Me <sub>3</sub> Si-GePh <sub>3</sub>	224 (2.2)	21
2 <i>t</i> -BuMe <sub>2</sub> Si-GePh <sub>3</sub>	229 (3.6)	21
3 Me <sub>3</sub> Si-Ge( <i>p</i> -Tol) <sub>3</sub> (1)	230 (3.3)	this work
4 Me <sub>3</sub> Ge-GePh <sub>3</sub>	230	8e
5 Me <sub>3</sub> Ge-Ge( <i>p</i> -Tol) <sub>3</sub> (2)	234 (3.7)	this work
6 Me <sub>3</sub> Sn-Ge( <i>p</i> -Tol) <sub>3</sub> (3)	240 (3.1)	this work
7 ( <i>p</i> -Tol) <sub>3</sub> Ge-GePh <sub>3</sub>	240	9
8 (Me <sub>3</sub> Si) <sub>3</sub> Ge-SiPh <sub>3</sub>	240 (4.4)	3b
9 (Me <sub>3</sub> Si) <sub>3</sub> Ge-GePh <sub>3</sub> (4)	234 (2.7)	this work
10 (Me <sub>3</sub> Si) <sub>3</sub> Ge-SnPh <sub>3</sub> (5)	242 (2.9)	this work
11 (Me <sub>3</sub> Si) <sub>3</sub> Ge-Sn(SiMe <sub>3</sub> ) <sub>3</sub>	214 (4.3)	3k
12 Ph <sub>3</sub> Ge-Ge(SiMe <sub>3</sub> ) <sub>2</sub> -GePh <sub>3</sub> (6)	245 (8.4)	this work
13 Ph <sub>3</sub> Ge-GeMe <sub>2</sub> -GePh <sub>3</sub>	245 (4.48)	22
14 Ph <sub>3</sub> Ge-GePh <sub>2</sub> -GePh <sub>3</sub>	249 (4.5)	12

It is evident that in the range of Si–Ge, Ge–Ge, and Sn–Ge derivatives the shift of UV absorption is observed. In the case of the tin compounds this shift is the most significant.

The same trend is observed for compounds 4 and 5. The tin compounds have red-shifted UV/visible spectra in comparison with Ge analogues.

A significant bathochromic shift is observed in trigermane 6 in comparison with digermane 4.

From the data given (Table 2, entries 1–3) it is evident that in compounds containing a Si–Ge fragment increasing the electron-donating properties of the substituents both at Si and at Ge results in a bathochromic shift. The same trend is observed for digermanes (Table 2, entries 4 and 5).

It should be noted that introduction of a tin atom in conjunction with Ge in any case results in a bathochromic shift, which may indicate the effective conjugation between Ge and Sn atoms. This shift is observed (Table 2, entries 3, 5, 6, and

8–11) in both Ar<sub>3</sub>M–GeAlk<sub>3</sub> and Ar<sub>3</sub>Ge–MAlk<sub>3</sub> series of compounds (M = Si, Ge, Sn). A more significant bathochromic shift is observed when only aromatic substituents are present on germanium atoms (Table 2, entries 5 and 7).

On comparison of (Me<sub>3</sub>Si)<sub>3</sub>Ge-SnPh<sub>3</sub> (4) and related compound (Me<sub>3</sub>Si)<sub>3</sub>Ge-Sn(SiMe<sub>3</sub>)<sub>3</sub>,<sup>3k</sup> an evident bathochromic shift on introduction of the aromatic substituents into the oligomeric chain is observed.

At the same time introduction of Si-containing groups to the central Ge atom in trigermanes (Table 2, entries 12–14) has a small effect on the spectral properties.

**Electrochemical Investigation.** Compounds 1–3 were investigated by cyclic voltammetry (Table 4, Figure 8; Figures S1–S4, Supporting Information). The measurements were performed in CH<sub>2</sub>Cl<sub>2</sub> using 0.1 M Bu<sub>4</sub>NBF<sub>4</sub> as a supporting electrolyte at different scan rates. All compounds have a peak in the anodic potential region corresponding to a one-electron (according to reference ferrocene oxidation, Figure S3) irreversible process. The oxidation is a diffusion-controlled process (inset in Figure S2). The irreversible oxidation in the case of 1–3 corresponds to data obtained earlier for related catenated compounds of the group 14 elements,<sup>20c–e,23</sup> but the reason for this irreversibility is not clear.<sup>8e</sup>

From the fact that the oxidation process is irreversible, it should be concluded that electron transfer is followed by chemical bond breaking (probably terminal Ge–E),<sup>24</sup> because this is the weakest bond in the compound (Scheme 4, eq 1). Cationic and radical particles are formed after this bond cleavage, and then the radical possibly abstracts an H atom from the solvent due to its high reactivity to form volatile HMMe<sub>3</sub>, which does not oxidize in the available potentials range.

The alternative oxidation mechanism including formation of a low-valent particle (germylene) has been postulated by Weinert et al.<sup>9</sup> (Scheme 4, eq 2). However, a cation radical generated as a result of the breaking of the Ge–M bond could oxidize germylene (Scheme 4, eq 3). The fact that germylene is not present in the products of 1–3 decomposition was proved earlier in a test trapping reaction with 1,3-dimethylbutadiene.<sup>8e</sup>

According to the data obtained, the oxidation potential increases in the series Ge–Sn < Ge–Ge < Ge–Si. Compounds 1–3 differ only in the nature of the element connected with the Ge(*p*-Tol)<sub>3</sub> fragment; thus the effect of substituents on electrochemical properties should be excluded. Therefore, it is the nature of the element (Si, Ge, Sn) that has a dramatic influence on the oxidation potentials. It should be proposed that the changes in ionization energies of the elements (which decreases in the order Si > Ge > Sn) play a key role. This sequence is correlated with the values of the oxidation potentials observed.

The value of the oxidation potential obtained for germanium compound 2 correlates well with those known for related compounds (Table 4).

**Luminescence.** The luminescence properties for oligogermanes are investigated only to a small degree. To the best of our knowledge, there are only several works in which polygermanes<sup>25</sup> or individual hexagermanes, (*i*-Pr)<sub>3</sub>Ge-(GePh<sub>2</sub>)<sub>4</sub>Ge(*i*-Pr)<sub>3</sub>,<sup>26</sup> have been investigated.

In this work it was established that compounds 1–3 exhibit fluorescence emission in solution (in CH<sub>2</sub>Cl<sub>2</sub>) and in the solid state (in powder) (Table 5, Figures 9, 10).

The characteristic Stokes shift is observed for the compounds studied. In the solid state there are three bands in the emission

Table 3. Data of the DFT Calculations for 1–4 and (Me<sub>3</sub>Si)<sub>3</sub>Ge-SiPh<sub>3</sub>

compound	$\lambda_{\max}$ (exp), nm	$\lambda_{\max}$ (calcd), nm <sup>a</sup>	$\Delta E(\text{HOMO-LUMO})$ , eV	transition
(p-Tol) <sub>3</sub> GeSiMe <sub>3</sub> (1)	230	244 (0.042)	7.28	HOMO → LUMO+2
		236 (0.239)		HOMO → LUMO+3
		234 (0.143)		HOMO → LUMO
		222 (0.055)		HOMO → LUMO+1
(p-Tol) <sub>3</sub> GeGeMe <sub>3</sub> (2)	232	229 (0.282)	7.48	HOMO → LUMO+2
		228 (0.186)		HOMO → LUMO
		215 (0.018)		HOMO → LUMO+1
(p-Tol) <sub>3</sub> GeSnMe <sub>3</sub> (3)	241	252 (0.056)	7.33	HOMO → LUMO
		242 (0.046)		HOMO → LUMO+3
		234 (0.264)		HOMO → LUMO+2
		233 (0.236)		HOMO → LUMO+1
(Me <sub>3</sub> Si) <sub>3</sub> GeSiPh <sub>3</sub>	240	252 (0.371)	8.01	HOMO → LUMO
		244 (0.071)		HOMO → LUMO+1
		241 (0.126)		HOMO → LUMO+2
		232 (0.080)		HOMO → LUMO+3
(Me <sub>3</sub> Si) <sub>3</sub> GeGePh <sub>3</sub> (4)	234	245 (0.234)	8.32	HOMO → LUMO
		238 (0.054)		HOMO → LUMO+1
		236 (0.115)		HOMO → LUMO+2
		228 (0.067)		HOMO → LUMO+3

<sup>a</sup>Oscillator strength in parentheses.

Table 4. Electrochemical Data for Compounds 1–3

compound	$E_{\text{ox}}$ (mV)	ref
Me <sub>3</sub> Si-Ge(p-Tol) <sub>3</sub> (1)	1790	this work
Me <sub>3</sub> Ge-Ge(p-Tol) <sub>3</sub> (2)	1650	this work
Me <sub>3</sub> Sn-Ge(p-Tol) <sub>3</sub> (3)	1520	this work
Me <sub>3</sub> Ge-GePh <sub>3</sub>	1795	8e
(n-Bu) <sub>3</sub> Ge-GePh <sub>3</sub>	1550	8e
(n-Hex) <sub>3</sub> Ge-GePh <sub>3</sub>	1515	8e

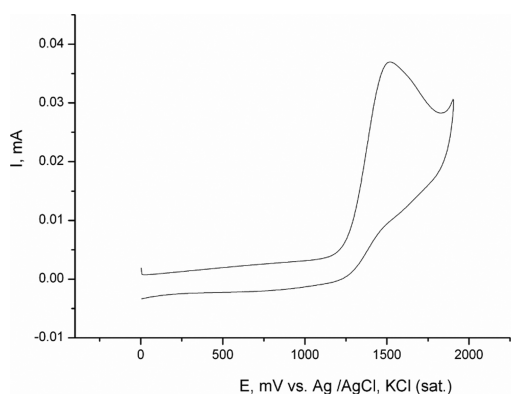


Figure 8. CV curve of a 1 M solution of compound 3 and (p-Tol)<sub>3</sub>Ge-SnMe<sub>3</sub> (CH<sub>2</sub>Cl<sub>2</sub>, 0.1 M Bu<sub>4</sub>NBF<sub>4</sub>, 100 mV/s, Pt).

#### Scheme 4. Possible Pathways of the Chemical Transformations of the Cation Radical Formed during Electrochemical Oxidation of Compounds 1–3

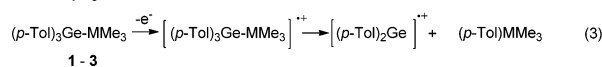
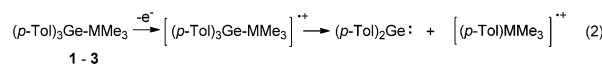
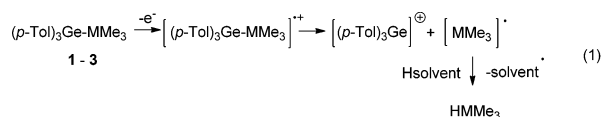


Table 5. Luminescence Emission Data for Compounds 1–3

compound	solid state		solution <sup>a</sup>	
	$\lambda_{\text{em}}$ (nm) <sup>b</sup>	$\lambda_{\text{em}}$ (nm) <sup>b</sup>	$\lambda_{\text{em}}$ (nm) <sup>b</sup>	$\Phi_{\text{f}}^{\text{c}}$ (%)
Me <sub>3</sub> Si-Ge(p-Tol) <sub>3</sub> (1)	357, 373, 393 (300)	284 (270)	5.64	
Me <sub>3</sub> Ge-Ge(p-Tol) <sub>3</sub> (2)	357, 373, 393 (300)	286 (270)	3.27	
Me <sub>3</sub> Sn-Ge(p-Tol) <sub>3</sub> (3)	361, 377, 397, 433 (315)	286 (270)	2.93	

<sup>a</sup>Spectra were recorded in CH<sub>2</sub>Cl<sub>2</sub>. <sup>b</sup>Excitation wavelength ( $\lambda_{\text{ex}}$ , nm) shown in parentheses. <sup>c</sup>Quantum yield.

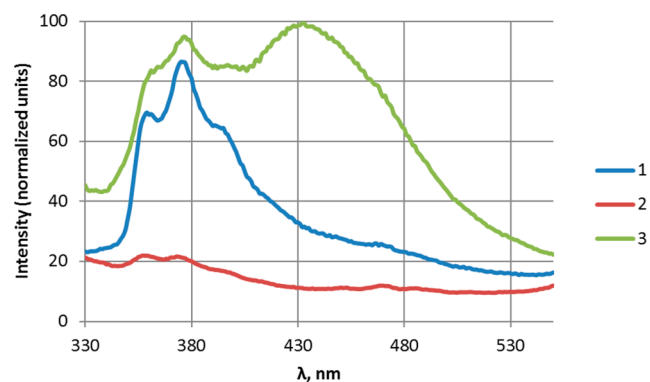
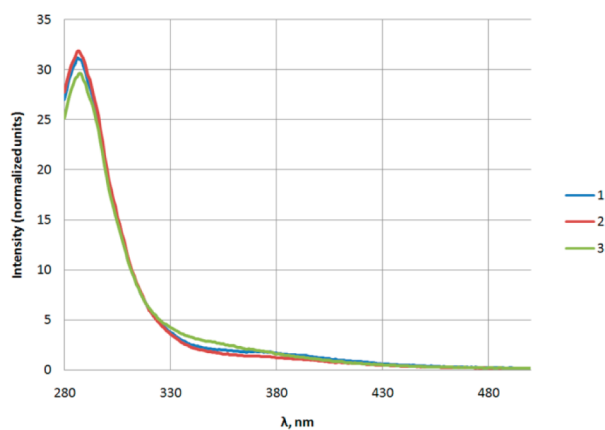


Figure 9. Fluorescence emission spectra for 1, 2 ( $\lambda_{\text{ex}}$  300 nm), and 3 ( $\lambda_{\text{ex}}$  315 nm) in the solid state.

spectra for 1–3, indicating several electron transitions. The first three bands are very similar (though a small shift to red field for the Sn derivative is observed) for all compounds. It should be noted that in the case of Ge (compound 2) fluorescence intensity is smaller than for other compounds studied, and for the tin compound the relative intensity is the largest. In solution compounds 1–3 have almost identical emission in terms of intensity and wavelength. But as shown in Table 5, all of the compounds have a low quantum yield, which decreases in the Si–Ge–Sn range.

Furthermore, in the case of compound 3 the additional band (433 nm) appears in the red field. Under more detailed



**Figure 10.** Fluorescence emission spectra for 1–3 ( $\lambda_{\text{ex}}$  270 nm) in solution in  $\text{CH}_2\text{Cl}_2$ .

investigation it was established that this band is caused by phosphorescence. The phosphorescence spectrum (Figure 11)

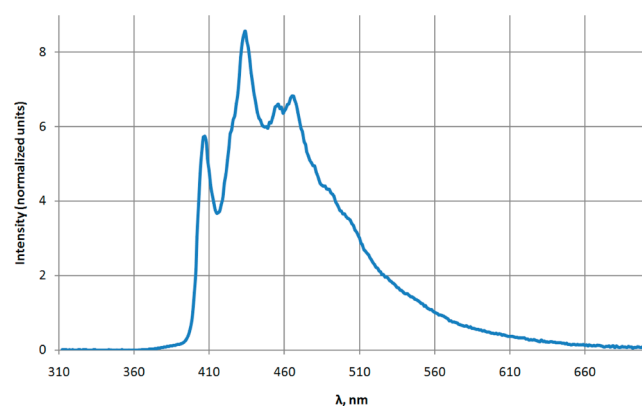


**Figure 11.** Phosphorescence spectrum for compound 3 ( $\lambda_{\text{ex}}$  300 nm,  $-196^\circ\text{C}$ , solid state).

contains several peaks, and the emission may be characterized by a very long lifetime (4.58 ms, Figure S5, Supporting Information). It may be proposed that phosphorescence is caused by Ge–Sn chromophore aggregation in the solid state.

To our knowledge this is a first example of phosphorescence of individual Ge-containing compounds.

**Theoretical Calculations.** The electronic gap and UV spectra of 1–4 and related  $(\text{Me}_3\text{Si})_3\text{Ge-SiPh}_3$  were investigated by DFT calculations and compared with experimental data (Table 3).

According to these data, the electronic transition occurs from the HOMO to the LUMO, LUMO+1, LUMO+2, and LUMO+3 orbitals. The orbitals for 4 are presented in Figure 12.

It is well established that the HOMO orbital is located on the central Ge–Si bond with a minor contribution from other molecule parts. On the contrary, the LUMO is mainly located on aromatic groups of  $\text{SiPh}_3$  with a high level of antibonding character, and the LUMO+1 and LUMO+2 are located only on aromatic groups. This situation in the case of compounds containing Si–Ge bonds is in accordance with digermanes studied earlier.<sup>8e</sup> In general the experimental data are in good agreement with theoretical calculations.

So it may be concluded that introduction of the electron-donating groups results in a bathochromic shift in the UV/visible spectra. Furthermore, substitution of the metal atom in

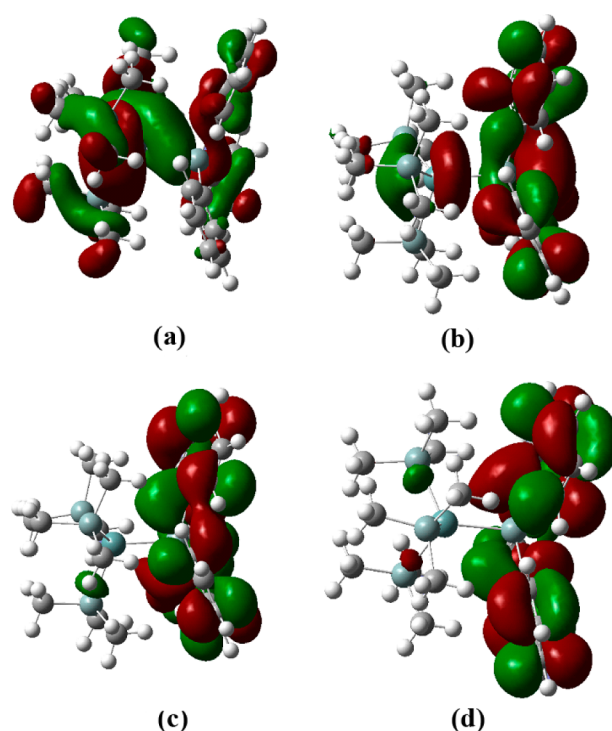


**Figure 12.** Graphical representation of HOMO (a), LUMO (b), LUMO+1 (c), and LUMO+2 (d) for compound  $(\text{Me}_3\text{Si})_3\text{Ge-SiPh}_3$ .

the series of compounds containing an M–M fragment in the range  $\text{Si} < \text{Ge} < \text{Sn}$  also results in a more significant red shift. In general, this shift is caused by the increasing overlap of the orbitals of Ge and Sn due to increased atomic size. Indeed, Wiberg indexes for model compounds  $\text{Ph}_3\text{Ge-MMe}_3$  ( $M = \text{Ge}$ , 0.743;  $M = \text{Sn}$ , 0.891) differ significantly. According to the NBO analysis, the hybridization in Ge–M differs, too. For tin derivatives the contribution of the s-orbital is increased, which should reduce the energy of the hybridized orbitals.

## CONCLUSIONS

In the course of this work two series of germanium compounds were obtained. It was established that the conditions of the reactions determine the nature of the products formed. Possible pathways of the chemical transformations of the cation radical formed during electrochemical oxidation of compounds 1–3 were proposed. Fluorescence emission for germanium compounds 1–3 in the solid state and in solution was found; tin compound 3 possesses phosphorescence in the solid state. The main result obtained in the course of this work is the fact that the introduction of tin-containing groups in conjugation with Ge results in a bathochromic shift in the UV/visible absorption.

## EXPERIMENTAL SECTION

**General Methods and Remarks.** All operations with germanium derivatives were conducted in a dry argon atmosphere using standard Schlenk techniques.  $^1\text{H}$  (400.130 MHz),  $^{13}\text{C}$  (100.613 MHz),  $^{29}\text{Si}$  (79.495 MHz), and  $^{119}\text{Sn}$  (149.211 MHz) NMR spectra were recorded on Bruker 400 or Agilent 400 spectrometers (at 295 K). Chemical shifts in the spectra are given in ppm relative to internal  $\text{Me}_4\text{Si}$  (for  $^1\text{H}$ ,  $^{13}\text{C}$ , and  $^{29}\text{Si}$  NMR) or  $\text{Me}_4\text{Sn}$  (for  $^{119}\text{Sn}$  NMR). Elemental analyses were carried out using a Heraeus Vario Elemental instrument. UV/visible spectra were recorded using a two-ray Evolution 300 spectrophotometer (Thermo Scientific) with a 0.10 cm long cuvette. Fluorescence (room temperature) and phosphor-

escence ( $-196\text{ }^{\circ}\text{C}$ ) spectra were recorded with a Hitachi F-7000 spectrofluorimeter. The fluorescence quantum yields were measured with respect to rhodamine. Voltammetric experiments were performed with an IPC-PRO potentiostat-galvanostat, in a handmade, one-compartment, 10 mL cell with a platinum wire counter electrode and Ag/AgCl/KCl aqueous reference electrode (RE). All potentials below refer to this reference electrode. The formal potential of the ferrocene couple (Fc/Fc<sup>+</sup>) versus our RE is about 0.6 V in (*n*-Bu)<sub>4</sub>NBF<sub>4</sub>/CH<sub>2</sub>Cl<sub>2</sub>. A Pt disk electrode with an active surface area of 0.049 cm<sup>2</sup> was used as the working electrode. Ohmic drop corrections were performed using the convolution approach. All solutions were thoroughly deaerated by passing an argon flow through the solution prior to the CV experiments and above the solution during the measurements; the supporting electrolyte in all experiments was 0.1 M (*n*-Bu)<sub>4</sub>NBF<sub>4</sub> (Aldrich, purity >99%), which had been dried under reduced pressure prior to use.

Solvents were dried using the usual procedures. Tetrahydrofuran and diethyl ether were stored under solid KOH and then distilled under sodium/benzophenone. Toluene, xylene (mixture of isomers), and *n*-hexane were refluxed and distilled under sodium. Dichloromethane was distilled under CaH<sub>2</sub>. C<sub>6</sub>D<sub>6</sub> was distilled over sodium under argon. CDCl<sub>3</sub> was distilled over CaH<sub>2</sub> under argon.

Mg (Aldrich), MeI (Aldrich), and *n*-BuLi (Aldrich) are commercial reagents and were used as received. (*p*-Tol)<sub>3</sub>GeH<sup>27</sup> and (Me<sub>3</sub>Si)<sub>4</sub>Ge<sup>28</sup> were synthesized according to literature procedures. Me<sub>3</sub>SiCl (Aldrich) was distilled over Al foil prior to use, and Me<sub>3</sub>SnCl (Aldrich) was recrystallized from *n*-hexane prior to use. *t*-BuOK (Aldrich) was sublimed (oil bath, 220 °C, 1 mmHg) prior to use and stored under argon.

**Synthesis of Compounds. Synthesis of Tetramethylgermane, Me<sub>4</sub>Ge.** An improved procedure was used.<sup>29</sup> A solution of MeI (160.00 g, 1.12 mol) in Et<sub>2</sub>O (150 mL) was added dropwise to a suspension of Mg (25.00 g, 1.03 mol) in Et<sub>2</sub>O (150 mL). Then the reaction mixture was refluxed for 1 h (requires using an efficient reflux condenser) and cooled to room temperature. Xylene (250 mL) was added to the reaction mixture, and the ether was distilled off. To an intensively stirring solution of the Grignard reagent obtained in xylene was added dropwise a solution of GeCl<sub>4</sub> (37.70 g, 0.176 mol) in xylene (50 mL) on cooling ( $-5$  to  $-10\text{ }^{\circ}\text{C}$ ). The mixture was slowly warmed to room temperature and then was refluxed for 6 h. Then the vessel was cooled, and the fraction with a bp of 40–100 °C was distilled out. This fraction was cooled in a two-necked flask (requires using an efficient reflux condenser), and then concentrated H<sub>2</sub>SO<sub>4</sub> was added dropwise. The organic phase was separated and purified by distillation. The Me<sub>4</sub>Ge was obtained as a colorless liquid (20.00 g, 90%), bp 43–44 °C,  $n_{\text{d}}^{20}$ , 1.3880. <sup>1</sup>H NMR (CDCl<sub>3</sub>, 400.130 MHz):  $\delta$  0.12 (s, CH<sub>3</sub>). <sup>13</sup>C{<sup>1</sup>H} NMR (CDCl<sub>3</sub>, 100.613 MHz):  $\delta$   $-0.68$  (CH<sub>3</sub>).<sup>30</sup>

**Synthesis of Trimethylbromogermane, Me<sub>3</sub>GeBr.** An improved procedure was used.<sup>31</sup> Me<sub>4</sub>Ge (50.00 g, 0.380 mol) and AlBr<sub>3</sub> (0.60 g, 2.25 mmol) were placed into a two-necked Erlenmeyer flask fitted with a thermometer and highly efficient reflux condenser. Then *i*-PrBr (46.10 g, 0.380 mol) was added dropwise. After the end of the reaction the reaction mixture was refluxed for 4 h until the vapor temperature reached 107–110 °C, and then the reaction mixture was fractionated. The Me<sub>3</sub>GeBr was obtained as a colorless liquid (57.00 g, 77%), bp 113–115 °C,  $n_{\text{d}}^{20}$ , 1.4635. <sup>1</sup>H NMR (CDCl<sub>3</sub>, 400.130 MHz):  $\delta$  0.83 (s, CH<sub>3</sub>). <sup>13</sup>C{<sup>1</sup>H} NMR (CDCl<sub>3</sub>, 100.613 MHz):  $\delta$  5.69 (CH<sub>3</sub>).

**Synthesis of Trimethyl[Tris(*p*-tolyl)germyl]silane, (*p*-Tol)<sub>3</sub>Ge-SiMe<sub>3</sub> (1).** *a. Synthesis of (*p*-Tol)<sub>3</sub>GeLi.* At room temperature a solution of *n*-BuLi in hexane (2.5 M, 0.58 mL, 1.44 mmol) was added dropwise to a solution of (*p*-Tol)<sub>3</sub>GeH (0.50 g, 1.44 mmol) in ether (20 mL). The reaction mixture was stirred for 6 h.

*b. Synthesis of (*p*-Tol)<sub>3</sub>Ge-SiMe<sub>3</sub> (1).* Me<sub>3</sub>SiCl (0.18 mL, 1.44 mmol) was added to a solution of (*p*-Tol)<sub>3</sub>GeLi in ether obtained earlier. The reaction mixture was stirred overnight. Then water (20 mL) was added, the organic phase was isolated, and the aqueous phase was extracted with ether (3 × 20 mL). The combined organic phase was dried over anhydrous Na<sub>2</sub>SO<sub>4</sub>, the volatiles were removed under vacuum, and the residue was recrystallized from *n*-hexane. Compound

1 was isolated as a white solid (0.58 g, 97%); mp 95–96 °C. <sup>1</sup>H NMR (CDCl<sub>3</sub>, 400.130 MHz):  $\delta$  7.39 (d, 6H, <sup>3</sup>J<sub>H-H</sub> = 7.8 Hz, aromatic protons); 7.21 (d, 6H, <sup>3</sup>J<sub>H-H</sub> = 7.8 Hz, aromatic protons); 2.41 (s, 9H, C<sub>6</sub>H<sub>4</sub>CH<sub>3</sub>), 0.38 (s, 9H, <sup>2</sup>J<sub>29Si-H</sub> = 3.3 Hz, SiMe<sub>3</sub>). <sup>13</sup>C{<sup>1</sup>H} NMR (CDCl<sub>3</sub>, 100.613 MHz):  $\delta$  137.81 (*ipso*-GeC<sub>6</sub>H<sub>4</sub>), 135.30 (*o*-GeC<sub>6</sub>H<sub>4</sub>), 135.00 (*p*-GeC<sub>6</sub>H<sub>4</sub>), 128.95 (*m*-H<sub>3</sub>CC<sub>6</sub>H<sub>4</sub>) (aromatic carbons); 21.40 (C<sub>6</sub>H<sub>4</sub>CH<sub>3</sub>);  $-0.33$  (SiMe<sub>3</sub>). <sup>29</sup>Si (CDCl<sub>3</sub>, 79.495 MHz):  $\delta$   $-10.40$  (SiMe<sub>3</sub>). Anal. Calcd for C<sub>24</sub>H<sub>30</sub>GeSi: C 68.77, H 7.21. Found: C 68.75, H 7.15. UV (CH<sub>2</sub>Cl<sub>2</sub>),  $\lambda_{\text{max}}$  nm ( $\epsilon$ , M<sup>-1</sup> cm<sup>-1</sup>): 231 (1.8 × 10<sup>4</sup>), 268 shoulder (0.1 × 10<sup>4</sup>). UV (*n*-hexane),  $\lambda_{\text{max}}$  nm ( $\epsilon$ , M<sup>-1</sup> cm<sup>-1</sup>): 230 (3.3 × 10<sup>4</sup>). Crystals suitable for single-crystal X-ray analysis were obtained under recrystallization from *n*-hexane at  $-30\text{ }^{\circ}\text{C}$ .

**Synthesis of 1,1,1-Trimethyl-3,3,3-(tris(*p*-tolyl)digermane, (*p*-Tol)<sub>3</sub>Ge-GeMe<sub>3</sub> (2).** The title compound was prepared analogously to compound 1 above using (*p*-Tol)<sub>3</sub>GeH (3.66 g, 10.60 mmol), *n*-BuLi in *n*-hexane (2.82 M, 3.90 mL, 11.00 mmol), and Me<sub>3</sub>GeBr (1.35 mL, 10.60 mmol). The crude substance was recrystallized from *n*-hexane. Compound 2 was isolated as a white solid (2.71 g, 55%); mp 97–98 °C. <sup>1</sup>H NMR (CDCl<sub>3</sub>, 400.130 MHz):  $\delta$  7.30 (d, 6H, <sup>3</sup>J<sub>H-H</sub> = 7.8 Hz, aromatic protons); 7.14 (d, <sup>3</sup>J<sub>H-H</sub> = 7.8 Hz, aromatic protons); 2.34 (s, 9H, C<sub>6</sub>H<sub>4</sub>CH<sub>3</sub>); 0.39 (s, 9H, GeMe<sub>3</sub>). <sup>1</sup>H NMR (C<sub>6</sub>D<sub>6</sub>, 400.130 MHz):  $\delta$  7.57 (d, 6H, <sup>3</sup>J<sub>H-H</sub> = 7.7 Hz, aromatic protons); 7.06 (d, <sup>3</sup>J<sub>H-H</sub> = 7.7 Hz, aromatic protons); 2.10 (s, 9H, C<sub>6</sub>H<sub>4</sub>CH<sub>3</sub>); 0.45 (s, 9H, GeMe<sub>3</sub>). <sup>13</sup>C{<sup>1</sup>H} NMR (CDCl<sub>3</sub>, 100.613 MHz):  $\delta$  138.03 (*ipso*-GeC<sub>6</sub>H<sub>4</sub>), 135.15 (*o*-GeC<sub>6</sub>H<sub>4</sub>), 134.74 (*p*-GeC<sub>6</sub>H<sub>4</sub>), 128.98 (*m*-H<sub>3</sub>CC<sub>6</sub>H<sub>4</sub>) (aromatic carbons); 21.41 (C<sub>6</sub>H<sub>4</sub>CH<sub>3</sub>);  $-0.86$  (GeMe<sub>3</sub>). <sup>13</sup>C{<sup>1</sup>H} NMR (C<sub>6</sub>D<sub>6</sub>, 100.613 MHz):  $\delta$  138.34 (*ipso*-GeC<sub>6</sub>H<sub>4</sub>), 135.66 (*o*-GeC<sub>6</sub>H<sub>4</sub>), 134.17 (*p*-GeC<sub>6</sub>H<sub>4</sub>), 129.51 (*m*-GeC<sub>6</sub>H<sub>4</sub>) (aromatic carbons); 21.32 (C<sub>6</sub>H<sub>4</sub>CH<sub>3</sub>);  $-0.81$  (GeMe<sub>3</sub>). Anal. Calcd for C<sub>24</sub>H<sub>30</sub>Ge<sub>2</sub>: C 72.90, H 6.12. Found: C 72.75, H 5.96. UV (CH<sub>2</sub>Cl<sub>2</sub>),  $\lambda_{\text{max}}$  nm ( $\epsilon$ , M<sup>-1</sup> cm<sup>-1</sup>): 232 (2.3 × 10<sup>4</sup>), 265 shoulder (0.1 × 10<sup>4</sup>). UV (*n*-hexane),  $\lambda_{\text{max}}$  nm ( $\epsilon$ , M<sup>-1</sup> cm<sup>-1</sup>): 234 (3.7 × 10<sup>4</sup>), 266 shoulder (0.1 × 10<sup>4</sup>). Crystals suitable for single-crystal X-ray analysis were obtained under recrystallization from *n*-hexane at  $-30\text{ }^{\circ}\text{C}$ .

**Synthesis of Tris(*p*-tolyl)(trimethylstannyl)germane, (*p*-Tol)<sub>3</sub>Ge-SnMe<sub>3</sub> (3).** The title compound was prepared analogously to compound 1 presented above using (*p*-Tol)<sub>3</sub>GeH (0.50 g, 1.44 mmol), *n*-BuLi in *n*-hexane (2.5 M, 0.58 mL, 1.44 mmol), and Me<sub>3</sub>SnCl (0.29 g, 1.44 mmol). The crude substance was recrystallized from an *n*-hexane/toluene mixture. Compound 3 was isolated as a white solid (0.47 g, 65%); mp 142–143 °C. <sup>1</sup>H NMR (CDCl<sub>3</sub>, 400.130 MHz):  $\delta$  7.33 (d, 6H, <sup>3</sup>J<sub>H-H</sub> = 7.8 Hz, aromatic protons); 7.18 (d, 6H, <sup>3</sup>J<sub>H-H</sub> = 7.8 Hz, aromatic protons); 2.37 (s, 9H, C<sub>6</sub>H<sub>4</sub>CH<sub>3</sub>); 0.32 (s, 9H, <sup>2</sup>J<sub>H-117Sn</sub> = 24.0 Hz, <sup>2</sup>J<sub>H-119Sn</sub> = 25.2 Hz, SnMe<sub>3</sub>). <sup>13</sup>C{<sup>1</sup>H} NMR (CDCl<sub>3</sub>, 100.613 MHz):  $\delta$  138.08 (*p*-GeC<sub>6</sub>H<sub>4</sub>), 135.51 (*ipso*-GeC<sub>6</sub>H<sub>4</sub>), <sup>2</sup>J<sub>13C-119Sn</sub> = 24.4 Hz, 135.10 (*m*-GeC<sub>6</sub>H<sub>4</sub>), <sup>4</sup>J<sub>13C-119Sn</sub> = 5.3 Hz, 129.06 (*o*-GeC<sub>6</sub>H<sub>4</sub>), <sup>3</sup>J<sub>13C-119Sn</sub> = 10.7 Hz (aromatic carbons); 21.41 (C<sub>6</sub>H<sub>4</sub>CH<sub>3</sub>);  $-9.76$  (SnMe<sub>3</sub>), <sup>1</sup>J<sub>13C-119Sn</sub> = 136.2 Hz). <sup>119</sup>Sn NMR (CDCl<sub>3</sub>, 149.211 MHz):  $\delta$   $-90.47$ . UV (CH<sub>2</sub>Cl<sub>2</sub>),  $\lambda_{\text{max}}$  nm ( $\epsilon$ , M<sup>-1</sup> cm<sup>-1</sup>): 241 (2.8 × 10<sup>4</sup>). UV (*n*-hexane),  $\lambda_{\text{max}}$  nm ( $\epsilon$ , M<sup>-1</sup> cm<sup>-1</sup>): 226 (3.6 × 10<sup>4</sup>), 240 (3.1 × 10<sup>4</sup>). Anal. Calcd for C<sub>24</sub>H<sub>30</sub>GeSn: C 56.54, H 5.93. Found: C 56.34, H 5.76.

**Synthesis of 1,1,1-Triphenyl-2,2,2-tris(trimethylsilyl)digermane, Ph<sub>3</sub>Ge-Ge(SiMe<sub>3</sub>)<sub>3</sub> (4).** *a. Synthesis of Tris(trimethylsilyl)germyl Potassium in THF.*<sup>3f</sup> Solid *t*-BuOK (0.95 g, 8.40 mmol) was added to a solution of (Me<sub>3</sub>Si)<sub>4</sub>Ge (3.03 g, 8.30 mmol) in THF (30 mL). The reaction mixture was stirred overnight, giving a yellowish solution.

*b. Synthesis of Ph<sub>3</sub>Ge-Ge(SiMe<sub>3</sub>)<sub>3</sub> (4) (Inverse Addition).* At  $-78\text{ }^{\circ}\text{C}$  a solution of (Me<sub>3</sub>Si)<sub>3</sub>GeK in THF prepared as described above was added slowly dropwise to a solution of Ph<sub>3</sub>GeCl (2.82 g, 8.30 mmol) in THF (40 mL). The reaction mixture was stirred overnight, and all volatile materials were removed under reduced pressure. The residue was purified by flash chromatography using petroleum ether as an eluent ( $R_f$  = 0.3). After recrystallization from *n*-hexane compound 4 (3.07 g, 62%) was obtained as a white powder; mp 242–243 °C, mp<sup>3f</sup> 97–99 °C. <sup>1</sup>H NMR (CDCl<sub>3</sub>, 400.130 MHz):  $\delta$  7.48–7.43 (m, 6H, aromatic protons); 7.35–7.28 (m, 9H, aromatic protons); 0.15 (s, 27H, <sup>2</sup>J<sub>H-29Si</sub> = 3.3 Hz, Ge(SiMe<sub>3</sub>)<sub>3</sub>). <sup>13</sup>C{<sup>1</sup>H} NMR (CDCl<sub>3</sub>, 100.613 MHz):  $\delta$  139.99 (*ipso*-C<sub>6</sub>H<sub>5</sub>), 135.51 (*o*-C<sub>6</sub>H<sub>5</sub>), 128.27 (*p*-C<sub>6</sub>H<sub>5</sub>),

127.93 (*m*-C<sub>6</sub>H<sub>5</sub>) (aromatic carbons); 3.24 (Si(CH<sub>3</sub>)<sub>3</sub>). <sup>29</sup>Si NMR (CDCl<sub>3</sub>, 79.495 MHz): δ -4.35 ppm. The NMR data in C<sub>6</sub>D<sub>6</sub> correspond to those given in the literature.<sup>3f</sup> UV (*n*-hexane), λ<sub>max</sub> nm (ε, M<sup>-1</sup> cm<sup>-1</sup>): 234 (2.7 × 10<sup>4</sup>).

**Synthesis of Triphenylstannyl[tris(trimethylsilyl)]germane, Ph<sub>3</sub>Sn-Ge(SiMe<sub>3</sub>)<sub>3</sub> (5).** *a. Synthesis of Tris(trimethylsilyl)germyl Potassium in the Presence of 18-Crown-6.*<sup>3j</sup> Toluene (50 mL) and 18-crown-6 (0.63 g, 2.38 mmol) were added to a mixture of *t*-BuOK (0.27 g, 2.41 mmol) and (Me<sub>3</sub>Si)<sub>4</sub>Ge (0.88 g, 2.41 mmol). The mixture was stirred overnight and then used without isolation.

*b. Synthesis of Ph<sub>3</sub>Sn-Ge(SiMe<sub>3</sub>)<sub>3</sub> (5).* At -78 °C a solution of (Me<sub>3</sub>Si)<sub>3</sub>GeK/18-crown-6 in toluene prepared as described above was added dropwise to a solution of Ph<sub>3</sub>SnCl (0.92 g, 2.39 mmol) in toluene (50 mL). The reaction mixture was stirred overnight, then diluted H<sub>2</sub>SO<sub>4</sub> (20 mL, 0.5 M) was added, the aqueous phase was extracted with ether (3 × 30 mL), the combined organic phases were dried over Na<sub>2</sub>SO<sub>4</sub>, the solvent was removed under reduced pressure, and the residue was recrystallized from *n*-hexane. Compound **5** (0.76 g, 52%) was isolated as a white powder; mp 158–160 °C. <sup>1</sup>H NMR (CDCl<sub>3</sub>, 400.130 MHz): δ 7.64–7.48 (m, 6H, *o*-C<sub>6</sub>H<sub>5</sub>), 7.37–7.30 (m, 9H, *m*- and *p*-C<sub>6</sub>H<sub>5</sub>); 0.24 (27H, Ge(SiMe<sub>3</sub>)<sub>3</sub>). <sup>13</sup>C{<sup>1</sup>H} NMR (CDCl<sub>3</sub>, 100.613 MHz): δ 141.38 (*ipso*-C<sub>6</sub>H<sub>5</sub>, <sup>1</sup>J<sub>13C-119Sn</sub> = 186.6 Hz), 137.38 (*o*-C<sub>6</sub>H<sub>5</sub>, <sup>2</sup>J<sub>13C-119Sn</sub> = 19.8 Hz), 128.23 (*m*-C<sub>6</sub>H<sub>5</sub>, <sup>3</sup>J<sub>13C-119Sn</sub> = 22.0 Hz), 128.20 (*p*-C<sub>6</sub>H<sub>5</sub>, <sup>4</sup>J<sub>13C-119Sn</sub> = 5.1 Hz), 3.53 (Ge(SiMe<sub>3</sub>)<sub>3</sub>, <sup>3</sup>J<sub>13C-119Sn</sub> = 7.3 Hz, <sup>1</sup>J<sub>13C-29Si</sub> = 22.7 Hz). <sup>29</sup>Si NMR (CDCl<sub>3</sub>, 79.495 MHz): δ -2.68. <sup>119</sup>Sn NMR (CDCl<sub>3</sub>, 149.211 MHz): δ -111.13 (<sup>2</sup>J<sub>29Si-119Sn</sub> = 20.7 Hz). UV (*n*-hexane), λ<sub>max</sub> nm (ε, M<sup>-1</sup> cm<sup>-1</sup>): 242 (2.9 × 10<sup>4</sup>). Anal. Calcd for C<sub>27</sub>H<sub>42</sub>GeSi<sub>3</sub>Sn: C 50.49, H 6.59. Found: C 50.27, H 6.53.

**Synthesis of 1,1,1,3,3,3-Hexaphenyl-2,2-bis(trimethylsilyl)-trigermane, Ph<sub>3</sub>Ge-Ge(SiMe<sub>3</sub>)<sub>2</sub>-GePh<sub>3</sub> (6).** *a. Synthesis of Tris(trimethylsilyl)germyl Potassium in THF.*<sup>3j</sup> Solid *t*-BuOK (0.32 g, 2.77 mmol) was added to a solution of (Me<sub>3</sub>Si)<sub>4</sub>Ge (1.01 g, 2.77 mmol) in THF (30 mL). The reaction mixture was stirred overnight, giving a yellowish solution.

*b. Synthesis of [Ph<sub>3</sub>Ge]<sub>2</sub>Ge(SiMe<sub>3</sub>)<sub>2</sub> (6) (Direct Addition).* At -78 °C a solution of Ph<sub>3</sub>GeCl (0.94 g, 2.77 mmol) in THF (40 mL) was added dropwise to a solution of (Me<sub>3</sub>Si)<sub>3</sub>GeK in THF prepared as described above. The reaction mixture was stirred overnight, and all volatile materials were removed under reduced pressure. The residue was purified by flash chromatography using petroleum ether as an eluent. The two fractions were isolated. The first fraction (*R*<sub>f</sub> = 0.3) is compound **4** (0.18 g, 32%). The second fraction (*R*<sub>f</sub> = 0.1) is compound **6**. After recrystallization from *n*-hexane/toluene (3:1) compound **6** (0.28 g, 36%) was obtained as a white powder; mp > 250 °C. <sup>1</sup>H NMR (CDCl<sub>3</sub>, 400.130 MHz): δ 7.33–7.20 (m, 18H, aromatic protons); 7.20–7.14 (m, 12H, aromatic protons); 0.12 (s, 27H, Ge(SiMe<sub>3</sub>)<sub>3</sub>). <sup>13</sup>C{<sup>1</sup>H} NMR (CDCl<sub>3</sub>, 100.613 MHz): δ 139.71 (*ipso*-C<sub>6</sub>H<sub>5</sub>), 135.73 (*o*-C<sub>6</sub>H<sub>5</sub>), 128.29 (*p*-C<sub>6</sub>H<sub>5</sub>), 127.84 (*m*-C<sub>6</sub>H<sub>5</sub>) (aromatic carbons); 3.67 (Si(CH<sub>3</sub>)<sub>3</sub>). <sup>29</sup>Si NMR (CDCl<sub>3</sub>, 79.495 MHz): δ -2.46 ppm. <sup>1</sup>H NMR (C<sub>6</sub>D<sub>6</sub>, 400.130 MHz): δ 7.54–7.47 (m, 12H, aromatic protons); 7.13–7.06 (m, 18H, aromatic protons); 0.28 (s, 27H, Ge(SiMe<sub>3</sub>)<sub>3</sub>) ppm. <sup>13</sup>C{<sup>1</sup>H} NMR (C<sub>6</sub>D<sub>6</sub>, 100.613 MHz): δ 140.24 (*ipso*-C<sub>6</sub>H<sub>5</sub>), 136.21 (*o*-C<sub>6</sub>H<sub>5</sub>), 128.76 (*p*-C<sub>6</sub>H<sub>5</sub>), 128.30 (*m*-C<sub>6</sub>H<sub>5</sub>) (aromatic carbons); 3.67 (Si(CH<sub>3</sub>)<sub>3</sub>). <sup>29</sup>Si NMR (C<sub>6</sub>D<sub>6</sub>, 79.495 MHz): δ -2.69. UV (CH<sub>2</sub>Cl<sub>2</sub>), λ<sub>max</sub> nm (ε, M<sup>-1</sup> cm<sup>-1</sup>): 247 (3.8 × 10<sup>4</sup>). UV (*n*-hexane), λ<sub>max</sub> nm (ε, M<sup>-1</sup> cm<sup>-1</sup>): 245 (8.4 × 10<sup>4</sup>). Crystals suitable for single-crystal X-ray analysis were obtained under recrystallization from toluene at -30 °C.

**Crystallography Details.** Experimental intensities for **1** and **6** were measured on a Bruker SMART APEX II diffractometer (graphite-monochromatized Mo K $\alpha$  radiation, λ = 0.710 73 Å); the data collection for **2** was performed on a STOE STADIVARI machine (graphite-monochromatized Cu K $\alpha$  radiation, λ = 1.541 86 Å). The structures were solved by direct methods and refined by full matrix least-squares on *F*<sup>2</sup> (SHELXTL) with anisotropic thermal parameters for all non-hydrogen atoms. All hydrogen atoms were placed in calculated positions and refined using a riding model. Details of X-ray experiments are given in Table S1.

**DFT Calculations.** The hybrid exchange–correlation functional using the Coulomb-attenuating method cam-B3LYP<sup>32</sup> has been used throughout the study because previous theoretical calculations have shown that the B3LYP approach is a cost-effective method for studying metal-containing systems.<sup>33</sup> Even with calculations of the thermodynamic parameters, B3LYP results compare well to the highly exact G2MP2 method, as well as to the experimental values.<sup>34</sup> We have used the DGDZVP basis set for all the atoms at the cam-B3LYP level. The DGDZVP basis set is an all-electron, double- $\zeta$  valence polarized basis set (for Si, Ge atoms) and the VDZP (valence double zeta + polarization) basis (for Sn atom), which were optimized specifically for DFT methods.<sup>35</sup> We have used the PM6 level for large systems with phenyl rings. Then optimized geometry was used for cam-B3LYP/DGDZVP calculations in single-point calculations. We have used the time-dependent density functional computations [6-311+G(d,p) basis set], as implemented by Gaussian 09, to explore the excited manifold and compute the possible electronic transitions.

The calculations were performed with full geometry optimization and used the GAUSSIAN'09 program package.<sup>36</sup> The absence of imaginary vibration frequencies confirmed the stationary character of the structures. The molecular orbitals and UV/visible spectra were constructed using the GaussView program. UV spectra were calculated in the approximate PCM (polarized continuum model)<sup>37</sup> in *n*-heptane.

## ■ ASSOCIATED CONTENT

### Supporting Information

CIF files giving crystallographic data for **1**, **2**, and **6**. The spectra of compounds obtained. A text file of all computed molecule Cartesian coordinates in a format for convenient visualization is present. The Supporting Information is available free of charge on the ACS Publications website at DOI: 10.1021/om501293t. The crystallographic data for **1**, **2**, and **6** have been deposited with the Cambridge Crystallographic Data Centre as supplementary publications under the CCDC numbers 1032425–1032427, respectively. They can be obtained free of charge from the Cambridge Crystallographic Data Centre via www.ccdc.cam.ac.uk/data\_request/cif.

## ■ AUTHOR INFORMATION

### Corresponding Author

\*Tel: +7(495)939 3887. Fax: +7(495)932-0067. E-mail: zaitsev@org.chem.msu.ru (K. V. Zaitsev).

### Notes

The authors declare no competing financial interest.

## ■ ACKNOWLEDGMENTS

This work was financially supported by the Russian President Grant for Young Russian Scientists (MK-1790.2014.3) and in part by M. V. Lomonosov Moscow State University Program of Development. We acknowledge Dr. M. V. Polyakova (MSU) for registration of UV spectra. We are grateful to Dr. S. V. Gruener (MSU) for his valuable advice and assistance in obtaining the initial germanes. We would like to thank the reviewers for their valuable comments.

## ■ REFERENCES

- (1) Amadoruge, M. L.; Weinert, C. S. *Chem. Rev.* **2008**, *108*, 4253–4294.
- (2) (a) Marschner, C.; Hlina, J. Catenated Compounds – Group 14 (Ge, Sn, Pb). In *Comprehensive Inorganic Chemistry II*, second ed.; Reedijk, J.; Poepplmeier, K., Eds. Elsevier: Amsterdam, 2013; pp 83–117. (b) Marschner, C.; Baumgartner, J. Disilanes and Oligosilanes. In *Science of Synthesis*; Oestreich, M., Ed.; Thieme Verlag: Stuttgart, 2013; pp 109–139. (c) Marschner, C., Oligosilanes. In *Functional Molecular*

*Silicon Compounds I*; Scheschkewitz, D., Ed.; Springer International Publishing, 2014; Vol. 155, pp 163–228.

(3) (a) Pannell, K. H.; Kapoor, R. N.; Raptis, R.; Párkányi, L.; Fülöp, V. *J. Organomet. Chem.* **1990**, *384*, 41–47. (b) Hlina, J.; Zitz, R.; Wagner, H.; Stella, F.; Baumgartner, J.; Marschner, C. *Inorg. Chim. Acta* **2014**, *422*, 120–133. (c) Schneider-Koglin, C.; Mathiasch, B.; Dräger, M. *J. Organomet. Chem.* **1993**, *448*, 39–46. (d) Sharma, H. K.; Cervantes-Lee, F.; Párkányi, L.; Pannell, K. H. *Organometallics* **1996**, *15*, 429–435. (e) Mallela, S. P.; Ghuman, M. A.; Geanangel, R. A. *Inorg. Chim. Acta* **1992**, *202*, 211–217. (f) Mallela, S. P.; Saar, Y.; Hill, S.; Geanangel, R. A. *Inorg. Chem.* **1999**, *38*, 2957–2960. (g) Mallela, S. P.; Geanangel, R. A. *Inorg. Chem.* **1994**, *33*, 1115–1120. (h) Müller, L.; du Mont, W. W.; Ruthe, F.; Jones, P. G.; Marsmann, H. C. *J. Organomet. Chem.* **1999**, *579*, 156–163. (i) Tice, J. B.; Chizmeshya, A. V. G.; Groy, T. L.; Kouvetakis, J. *Inorg. Chem.* **2009**, *48*, 6314–6320. (j) Fischer, J.; Baumgartner, J.; Marschner, C. *Organometallics* **2005**, *24*, 1263–1268. (k) Baumgartner, J.; Fischer, R.; Fischer, J.; Wallner, A.; Marschner, C.; Flörke, U. *Organometallics* **2005**, *24*, 6450–6457. (l) Hlina, J.; Mechtler, C.; Wagner, H.; Baumgartner, J.; Marschner, C. *Organometallics* **2009**, *28*, 4065–4071. (m) Emanuelsson, R.; Denisova, A. V.; Baumgartner, J.; Ottosson, H. *Organometallics* **2014**, *33*, 2997–3004.

(4) Zaitsev, K. V.; Kapranov, A. A.; Churakov, A. V.; Poleshchuk, O. K.; Oprunenko, Y. F.; Tarasevich, B. N.; Zaitseva, G. S.; Karlov, S. S. *Organometallics* **2013**, *32*, 6500–6510.

(5) Harloff, J.; Popowski, E.; Fuhrmann, H. *J. Organomet. Chem.* **1999**, *592*, 136–146.

(6) Párkányi, L.; Hernandez, C.; Pannell, K. H. *J. Organomet. Chem.* **1986**, *301*, 145–151.

(7) Kawachi, A.; Tanaka, Y.; Tamao, K. *J. Organomet. Chem.* **1999**, *590*, 15–24.

(8) (a) Bochkova, R. I.; Drozdov, Y. N.; Kuzmin, E. A.; Bochkarev, L. N.; Bochkarev, M. N. *Russ. J. Coord. Chem. (in Russ.)* **1987**, *13*, 1126–1129. (b) Parkanyi, L.; Kalman, A.; Sharma, S.; Nolen, D. M.; Pannell, K. H. *Inorg. Chem.* **1994**, *33*, 180–182. (c) Subashi, E.; Rheingold, A. L.; Weinert, C. S. *Organometallics* **2006**, *25*, 3211–3219. (d) Amadoruge, M. L.; Di Pasquale, A. G.; Rheingold, A. L.; Weinert, C. S. *J. Organomet. Chem.* **2008**, *693*, 1771–1778. (e) Schrick, E. K.; Forget, T. J.; Roewe, K. D.; Schrick, A. C.; Moore, C. E.; Golen, J. A.; Rheingold, A. L.; Materer, N. F.; Weinert, C. S. *Organometallics* **2013**, *32*, 2245–2256.

(9) Amadoruge, M. L.; Short, E. K.; Moore, C.; Rheingold, A. L.; Weinert, C. S. *J. Organomet. Chem.* **2010**, *695*, 1813–1823.

(10) Ng, M. C. C.; Craig, D. J.; Harper, J. B.; Eijck, L.; Stride, J. A. *Chem.–Eur. J.* **2009**, *15* (27), 6569–6572.

(11) (a) Zirngast, M.; Flock, M.; Baumgartner, J.; Marschner, C. *J. Am. Chem. Soc.* **2009**, *131*, 15952–15962. (b) Sekiguchi, A.; Fukaya, N.; Ichinohe, M.; Takagi, N.; Nagase, S. *J. Am. Chem. Soc.* **1999**, *121*, 11587–11588. (c) Sekiguchi, A.; Yamazaki, H.; Kabuto, C.; Sakurai, H.; Nagase, S. *J. Am. Chem. Soc.* **1995**, *117*, 8025–8026. (d) Mallela, S. P.; Hill, S.; Geanangel, R. A. *Inorg. Chem.* **1997**, *36*, 6247–6250.

(12) Roller, S.; Simon, D.; Dräger, M. *J. Organomet. Chem.* **1986**, *301*, 27–40.

(13) Dräger, M.; Simon, D. *J. Organomet. Chem.* **1986**, *306*, 183–192.

(14) Haberle, K.; Dräger, M. *J. Organomet. Chem.* **1986**, *312*, 155–165.

(15) Weidenbruch, M.; Hagedorn, A.; Peters, K.; von Schnering, H. *G. Angew. Chem., Int. Ed. Engl.* **1995**, *34*, 1085–1086.

(16) Weidenbruch, M.; Hagedorn, A.; Peters, K.; von Schnering, H. *G. Chem. Ber.* **1996**, *129*, 401–404.

(17) Weinhold, F.; Landis, C. L. *Valency and Bonding: A Natural Donor-Acceptor Perspective*, 1st ed.; Cambridge University Press, 2005.

(18) Miller, R. D.; Michl, J. *Chem. Rev.* **1989**, *89*, 1359–1410.

(19) (a) Marschner, C.; Baumgartner, J.; Wallner, A. *Dalton Trans.* **2006**, 5667–5674. (b) Wallner, A.; Hlina, J.; Wagner, H.; Baumgartner, J.; Marschner, C. *Organometallics* **2011**, *30*, 3930–3938.

(20) (a) Zaitsev, K. V.; Kapranov, A. A.; Oprunenko, Y. F.; Churakov, A. V.; Howard, J. A. K.; Tarasevich, B. N.; Karlov, S. S.; Zaitseva, G. S. *J. Organomet. Chem.* **2012**, *700*, 207–213. (b) Amadoruge, M. L.;

Golen, J. A.; Rheingold, A. L.; Weinert, C. S. *Organometallics* **2008**, *27*, 1979–1984. (c) Amadoruge, M. L.; Gardiner, J. R.; Weinert, C. S. *Organometallics* **2008**, *27*, 3753–3760. (d) Samanamu, C. R.; Amadoruge, M. L.; Yoder, C. H.; Golen, J. A.; Moore, C. E.; Rheingold, A. L.; Materer, N. F.; Weinert, C. S. *Organometallics* **2011**, *30*, 1046–1058. (e) Samanamu, C. R.; Amadoruge, M. L.; Schrick, A. C.; Chen, C.; Golen, J. A.; Rheingold, A. L.; Materer, N. F.; Weinert, C. S. *Organometallics* **2012**, *31*, 4374–4385.

(21) Zaitsev, K. V.; Oprunenko, Y. F.; Churakov, A. V.; Zaitseva, G. S.; Karlov, S. S. *Main Group Met. Chem.* **2014**, *37*, 67–74.

(22) Castel, A.; Riviere, P.; Saintroch, B.; Satge, J.; Malrieu, J. P. *J. Organomet. Chem.* **1983**, *247*, 149–160.

(23) (a) Okano, M.; Mochida, K. *Chem. Lett.* **1990**, 701–704.

(b) Mochida, K.; Hodota, C.; Hata, R.; Fukuzumi, S. *Organometallics* **1993**, *12*, 586–588.

(24) Mochida, K.; Chiba, H.; Okano, M. *Chem. Lett.* **1991**, *20*, 109–112.

(25) Huo, Y.; Berry, D. H. *Chem. Mater.* **2005**, *17*, 157–163.

(26) Roewe, K. D.; Rheingold, A. L.; Weinert, C. S. *Chem. Commun.* **2013**, *49*, 8380–8382.

(27) Lee, V. Y.; Yasuda, H.; Ichinohe, M.; Sekiguchi, A. *J. Organomet. Chem.* **2007**, *692*, 10–19.

(28) Brook, A. G.; Abdesaken, F.; Söllradl, H. *J. Organomet. Chem.* **1986**, *299*, 9–13.

(29) Nаметкин, N. S.; Durgaryan, S. G.; Tikhonova, L. I. *Dokl. Akad. Nauk SSSR (in Russ.)* **1967**, *172*, 615–617.

(30) Liepiņš, E.; Petrova, M. V.; Bogoradovsky, E. T.; Zavgorodny, V. S. *J. Organomet. Chem.* **1991**, *410*, 287–291.

(31) Mironov, V. F.; Kravchenko, A. L. *Bull. Acad. Sci. USSR Div. Chem. Sci. (Engl. Transl.)* **1965**, *14*, 988–995.

(32) Yanai, T.; Tew, D. P.; Handy, N. C. *Chem. Phys. Lett.* **2004**, *393*, 51–57.

(33) Poleshchuk, O. K.; Shevchenko, E. L.; Branchadell, V.; Lein, M.; Frenking, G. *Int. J. Quantum Chem.* **2005**, *101*, 869–877.

(34) Curtiss, L. A.; Raghavachari, K.; Redfern, P. C.; Pople, J. A. *J. Chem. Phys.* **1997**, *106*, 1063–1079.

(35) (a) Godbout, N.; Salahub, D. R.; Andzelm, J.; Wimmer, E. *Can. J. Chem.* **1992**, *70*, 560–571. (b) Sosa, C.; Andzelm, J.; Elkin, B. C.; Wimmer, E.; Dobbs, K. D.; Dixon, D. A. *J. Phys. Chem.* **1992**, *96*, 6630–6636.

(36) Frisch, M. J.; Trucks, G. W.; Schlegel, H. B.; Scuseria, G. E.; Robb, M. A.; Cheeseman, J. R.; Scalmani, G.; Barone, V.; Mennucci, B.; Petersson, G. A.; Nakatsuji, H.; Caricato, M.; Li, X.; Hratchian, H. P.; Izmaylov, A. F.; Bloino, J.; Zheng, G.; Sonnenberg, J. L.; Hada, M.; Ehara, M.; Toyota, K.; Fukuda, R.; Hasegawa, J.; Ishida, M.; Nakajima, T.; Honda, Y.; Kitao, O.; Nakai, H.; Vreven, T.; Montgomery, J. A.; Peralta, J. E.; Ogliaro, F.; Bearpark, M.; Heyd, J. J.; Brothers, E.; Kudin, K. N.; Staroverov, V. N.; Kobayashi, R.; Normand, J.; Raghavachari, K.; Rendell, A.; Burant, J. C.; Iyengar, S. S.; Tomasi, J.; Cossi, M.; Rega, N.; Millam, J. M.; Klene, M.; Knox, J. E.; Cross, J. B.; Bakken, V.; Adamo, C.; Jaramillo, J.; Gomperts, R.; Stratmann, R. E.; Yazyev, O.; Austin, A. J.; Cammi, R.; Pomelli, C.; Ochterski, J. W.; Martin, R. L.; Morokuma, K.; Zakrzewski, V. G.; Voth, G. A.; Salvador, P.; Dannenberg, J. J.; Dapprich, S.; Daniels, A. D.; Farkas, O.; Foresman, J. B.; Ortiz, J. V.; Cioslowski, J.; Fox, D. J. *GAUSSIAN'09*; Gaussian, Inc.: Wallingford, CT, 2009.

(37) Tomasi, J.; Persico, M. *Chem. Rev.* **1994**, *94*, 2027–2094.